Journal of Multidisciplinary Engineering Science and Technology (JMEST)
ISSN: 2458-9403
Vol. 6 Issue 1, January - 2019

Impact Of Casting Process Conditions On The Structure And Ductility Of An AHSS Steel Slab

Marina Flaman
Process Technology Group: Metallurgy
Department - DEYTEMA Center
Universidad Tecnológica Nacional
Facultad Regional San Nicolás
San Nicolás, Argentina
mflaman@frsn.utn.edu.ar

Elena Brandaleze
Process Technology Group: Metallurgy
Department - DEYTEMA Center
Universidad Tecnológica Nacional
Facultad Regional San Nicolás
San Nicolás, Argentina
ebrandaleze@frsn.utn.edu.ar

***Abstract*—The current challenge in the steel industry is to increase the quality of steel products. In this sense it is necessary to avoid defects in steel semi-finished products (slabs) as well as to develop good control on primary production technology, especially in the continuous casting conditions. For automotive steel sheet grades, the main requirements are good formability, combining high strength and ductility. Hot stamping process is used to manufacture light weight steel car body parts. Advanced High Strength Steels (AHSS) such as boron steels, are the most used for hot stamping.**

Low boron additions to the steel composition improve mechanical properties, provide hardenability and weight savings compared with conventional steels. Boron in these steels should remain free (in solid solution), avoiding precipitates generation in the structure. During solidification in the continuous casting, alterations of the process conditions can promote product defects and produce ductility loss. The paper presents results of a study conducted on boron steel slab which includes sample characterization applying non-destructive tests (ultrasonic and penetrant liquid tests) in order identify the presence of defects in the product correlated with a structural study using different microscopy techniques, hardness and microhardness measurements. Information of localized mechanical properties of the slab sample was obtained. In addition, a thermodynamic simulation using FactSage 7.2 was carried out to get information on boron nature in the steel structure and the type of precipitates formed at different cooling temperature conditions. The information is considered very useful for processing AHSS steel through continuous casting.

Keywords—AHSS steel; casting conditions; thermodynamic simulation; solidification process

I. INTRODUCTION

In the automotive industry, conventional High Strength Low Alloy steels (HSLA) with a good combination of ductility and strength are increasingly being replaced by Advanced High Strength Steels (AHSS) with a multiphase structure. In the context of multiphase steels, boron is the unique alloy element that in a soluble content of 0.0010%-0.0030% can provide a hardenability effect equivalent to adding 0.5% of other elements (Mn, Cr and Mo) with a good mechanical behaviour. For this reason, the steel industry is interested in producing multiphase boron steel which makes it possible to reduce costs [1].

Hot stamping process of steel car body parts requires steel products of a very high quality. Slabs produced by continuous casting must be free of shrinkage, porosity, segregation or cracks. Therefore, it is necessary to improve the production technology of this type of slab, to choose the best casting temperature, to optimize the regime of mould filling, and also to verify the ratio, the chamfer and the external/internal shape of the mold wall to minimize defects [2]. Aligned with the points mentioned, it is relevant to take into account the liquidus temperature of the steel (T_L) that is considered an important variable to correlate with the solidification process conditions. The Irving empirical expression (1) allows to approximate T_L temperature on the base of steel chemical composition [3].

$$T_L\,(°C) = 1536 - [78\%C + 7{,}6\%Si + 4{,}9\%Mn + 34\%P + 30\%S + 18\%Ti] \quad (1)$$

Also, it is important to increase the knowledge on the nature of boron in the steel structure in relation with temperature, the impact of phase transformation and the types of precipitates formed at cooling conditions during the solidification process, in order to predict the mechanical behaviour and probable ductility loss. Continuous casting is commonly carried out in a curved mold with the strand being straightened when the steel has solidified throughout its cross section. This straightening or unbending operation causes tension in the top surface of the strand. The unbending temperature falls in the temperature range between 1100ºC - 700 ºC, in which it is important to warrant good hot ductility. Therefore, the combination of low ductility and a tensile strain may cause cracking in the product. Thermodynamic simulation applying Fact Sage, is considered a good tool that provides useful information on the steel system, boron nature and of the precipitation phenomena at different

temperature process conditions [4, 5]. This paper present results of a study carried out on an AHSS steel slab sample.

The main objective is to predict the structural evolution during cooling in the continuous casting process, to determine the causes of the superficial and internal defects in order to modify the process conditions that make it possible to improve the quality of steel boron slabs. Moreover, the study provides information on phase transformation and precipitation phenomena in relation with temperature, which could affect hot ductility during cooling. Sample characterization includes nondestructive tests (ultrasonic and penetrant liquid), a structural study by optical microscopy and scanning electron microscopy (SEM) with EDS analysis, hardness and microhardness measurements in different sample zones. Finally, based on the steel chemical composition, thermodynamic simulations of the structural changes and precipitation phenomena were carried out using the software FactSage 7.2, applying the methodology described by Brandaleze E. et al. [5]. The information is useful to predict hot ductility loss and cracking problems at continuous casting conditions.

II. Methodology

A transversal steel slab sample was selected for the structural characterization. In order to observe the structure and to identify the presence of defects in the as cast product, first of all the sample was cleaned and etched with HCL (50% v/v at 90ºC) to observe the primary solidification structure. Then the sample was divided in three zones: surface zone (SZ), medium zone (MZ) and centre zone (CZ). Non-destructive tests were carried out together with a visual inspection in different zones of the sample. Two tests were performed in order to identify defects: a penetrant liquid test applying spray Magnaflux (type II visible penetrant, method C solvent removable and type e non aqueous developer), and an ultrasonic test using a Phasor XS, General Electric equipment with 3 transductors: 2 single crystal straight-beam (24 mm, 4 MHz y 1MHz) and 1 dual crystal straight-beam (2 MHz), The structural study included optical microscopy observations using an OLYMPUS GX 51 microscope with a Leco IA32 image analyzer system and also scanning electron microscopy (SEM+EDS) applying a FEI Quanta 200 instrument. The mechanical behaviour of the sample was established through hardness measurements performed by a CIFIC/EQUOTIP durometer and microhardness tests carried out in the three zones (SZ, MZ and CZ) by a Leco LM300AT, with a load of 25 g. Each average microhardness value was determined based on 10 measurements. The thermodynamic simulation, was performed by the software FactSage 7.2. This tool provides information about phase transformations and precipitation processes that can occur at cooling conditions. In agreement with [4, 5], the simulation was carried out in the range of 1550 ºC - 400 ºC, applying the Equilib module and FSteel and Misc data bases.

III. Results and discussion

Advanced High Strength Steels (AHSS) are being used increasingly in many automotive parts replacing HSLA steels due to their more desirable strength-ductility ratio. The steel selected for this study, is a B-Ti steel with high boron content (≅ 42 ppm B and 32 ppm of N), see Table I.

TABLE I. Steel Chemical Composition

%C	%Mn	%Si	%Ti	%P	%S
0.30	1.46	0.17	0.035	0.015	0.0039
%B	**%N**				
0.0042	0.0032				

Boron additions in steel affects the austenite transformation during cooling and controls the final amount of bainite in the multiphase structure. Murari in [1], confirm that ≅ 27 ppm of boron exhibited a good impact on the mechanical behavior. Ti addition to these grades carried out to promote TiN precipitation, which acts as a grain growth inhibitor, improves mechanical properties and prevents BN precipitation. Ti also affects the ductility temperature range of B-Ti steels during cooling in the continuous casting process [6].

The knowledge and optimization of the existing casting parameters, such as: casting speed and casting temperature of steel, are the main preconditions for steel slab defects minimization, especially porosity, macrosegregation and cracks. Porosity is induced by two types of mechanisms: solidification shrinkage and gas segregation [2]. Cracks can grow during subsequent deformations owing to thermal gradients, ferrostatic pressure of liquid, and rolls misalignment. In addition to the cracking in the mould, there is also a problem of cracking during slab straightening at the end of the continuous casting process. This is associated with low hot ductility in steel. For this reason it is important to take into account the main solidification process conditions of the sample. The operation parameters applied during slab casting were: cast temperature T_c=1530ºC and casting speed c_s=1 m/min. The liquidus temperature of the boron steel estimated by (1) is T_L= 1502ºC. The value indicates that the steel during casting process is at 28 degrees above the liquidus temperature.

A. Non-destructive tests

Ultrasonic tests were carried out in different zones of the slab sample applying a Phasor XS ultrasonic device and three different transducers: two normal beams (24 mm, 4 MHz and 1MHz) and a dual element transducer (2 MHz). The results obtained with the

normal beam transducer (24mm-4MHz) are considered the most suitable for this case study. Instrument calibration was carried out following the parameters indicated in Table II, according with the specification for straight - beam ultrasonic examination of steel plates SA-435/SA-435M. The scanning was performed in different zones of the slab sample with a test frequency and instrument adjustment that produce a minimum at 50% and a maximum at 75%, at full scale.

TABLE II. CALIBRATION PARAMETERS.

Parameter	Value
Applied gain	43,8 dB
Range	50 mm
Rate	5704 m/s

In the sample CZ (slab centre), an important decrease of the back reflection was obtained. This result could be explained by the presence of central porosity and/or the characteristics of the casting structure present in the slab sample centre. *Fig. 1. Shows the image of the screen with the ultrasonic signal waves obtained in slab sample CZ zone.*

Important cracks in MZ zone (intermediate slab zone) of the sample were detected through the decrease of the back-reflection intensity to almost zero and "noise" on screen was observed. The reason could be the air retained inside the cracks that absorbs a significant proportion of the ultrasonic energy wave. As described in [7], non-destructive tests (NDT) such as ultrasonic signals are practical, economical and an increasingly used method, for examining bulk defects in slabs. These results are complemented with a systematic microstructural analysis. Samples that are examined by NDT can go directly to the hot rolling process avoiding special changes in the normal production line.

By means of penetrant tests, it was possible to corroborate and identify defects present in the transversal slab sample. Surface cracks were observed in the shell (SZ zone). Cracks detected by ultrasonic test in MZ zone, were also corroborated through a penetrant test. In the center of the slab (CZ zone) porosity associated with segregation was clearly visualized.

Surface cracks in continuous casting can be classified in: cracks which occur during solidification and those which occur after solidification of the steel shell. Stresses developed during the cooling process are the main cause in both cases [8]. *Fig. 2* shows the cracks appearance observed in MZ zone through penetrant test.

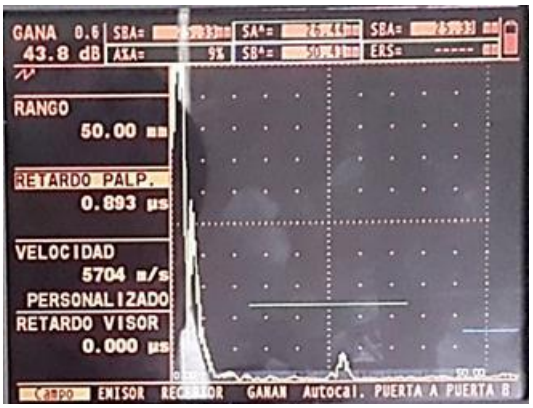

Fig. 1. *Screen of the ultrasonic instrument showing the signal waves obtained in CZ zone of the slab sample.*

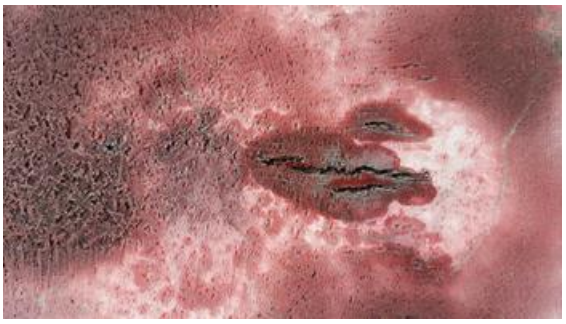

Fig. 2. *Cracks revealed by penetrant liquid test in MZ zone of the slab sample.*

B. Structural characterization

Through macro etchant (HCL 50% v/v at 90ºC) the casting structure was observed and the mentioned defects present in slab were corroborated and localized in relation with the structure characteristics. Surface cracks (at SZ zone) present different causes [8]: a) early δ/γ transformation in the initial shell which induced air gap formation and hence uneven growth of the shell with local temperature rise b) hot ductility problems at the straightening stage. In this case study, the second cause makes it possible to justify the surface cracks which are oriented along the direction of compression imposed during solidification. Straightening stage occurs at temperature ≤ 1000°C and imposes a tensile strain on the top surface of slab promoting the surface cracks observed in the slab sample. Cracks present in MZ zone, show a clear propagation aligned with the direction of dendrites growth. Both problems, segregation combined with central porosity, were verified by macro etchant in CZ zone of the slab. Furthermore, samples SZ, MZ and CZ (etched with Nital 2%), were observed by optical microscopy. In SZ and MZ samples, some inclusions and important quantity of precipitates with spherical or irregular shape were identified in the grain boundaries and within the grains. Also, ultrafine precipitates were observed within the grains. *Fig. 3 and 4* show the precipitates present in dendritic grain boundaries and within the grains in MZ sample.

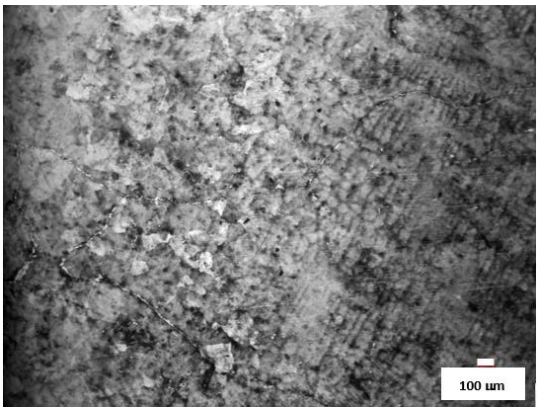

Fig. 3. *Precipitates present in dendrite grain boundaries and within grains.*

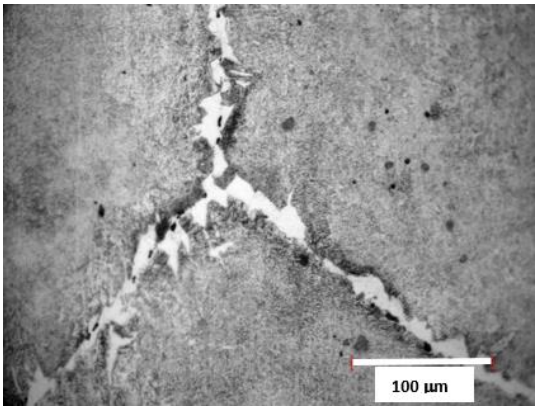

Fig. 4. *Detail of precipitates spherical or irregular shape observed.*

In the slab centre sample (CZ) porous of different sizes associated with segregation, were observed. *Fig. 5*

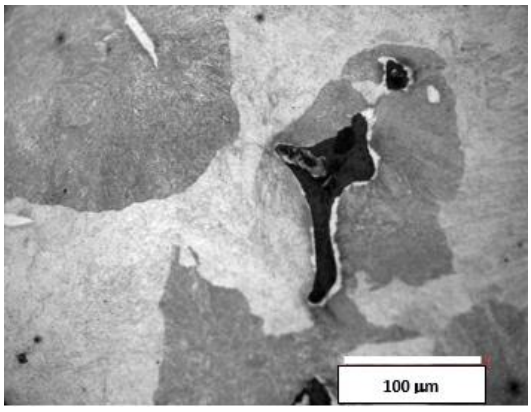

Fig. 5. *Porous of different sizes observed in CZ sample.*

Segregation or enrichment of solutes and alloying elements is the most important phenomenon occurring during the solidification of steel. When solute concentration in the interdendritic liquid becomes sufficiently high, reactions may occur between the solutes resulting in the formation of inclusions (oxides, silicates, oxysulphides) and gas bubbles. An important reaction in the impurity enriched interdendritic liquid is the precipitation of MnS inclusions [8]. The central porosity observed could be justified by casting parameters alteration such as: casting temperature, excessive refrigeration in the mold or in the secondary refrigeration zone and pressure changes in the extraction rolls during solidification. The structural study was completed by scanning electron microscopy SEM including semiquantitative EDS analysis, to identify inclusions and precipitates present in different zones of the slab sample. In the shell structure (SZ zone), the precipitates identified and corroborated by EDS analysis are: CNTi, CS_2Ti and TiC. TiC are associated with complex silicates inclusions (size≈ 5µm). In agreement with [9], a considerable quantity of MnS type I and II inclusions with globular or elongated morphology, was determined. These types of MnS are considered deformable. Globular MnS (type I) is formed by a monotectic reaction when the oxygen solubility is high and the sulfur solubility is low. MnS type II precipitates are formed in the interdendritic spaces of austenite with elongated or fan-like morphology. In both zones (medium MZ and centre CZ) of the slab: TiC, CNTi and CS_2Ti precipitates are also present and associated to complex inclusions. Besides, MnS type II (deformables) and type III (polygonals) were determined. MnS type III appear isolated in the interdendritic spaces of austenite and may be more harmful for mechanical properties [9]. The precipitation of MnS inclusions occurs especially during the later stages of solidification by reactions in the interdendritic liquid because of the impurity enrichment. In the vicinity of the liquidus temperature T_L (in this case 1502°C), the solid MnS solubility product [%Mn][%S] is about 0.92. For high casting speed and a ratio Mn/S $>$ 0.92 a more favorable reaction could generate FeS, resulting in hot ductility loss. The casting speed in this case study was c_s=1 m/min. However the structural study did not reveal FeS precipitates in the last liquid freezing at casting conditions used. Si and Al reduces liquid iron surface tension, modifying the solidification conditions and elements segregation (Si and P) in a more fluid interdendritic liquid. Deformation during solidification causes the structure to be subjected to a compressive longitudinal deformation and to be swelled out horizontally, owing to the internal hydrostatic pressure. In consequence, liquid is pushed between grains interphases accumulating particles and inclusions at grain boundaries leading to severely weakened grain boundaries. A highly segregated liquid is compressed and sheared between horizontal grains leading to grain boundary cracks (intergranular cracks) upon completion of solidification [8]. Roll misalignment and bending of the semisolid strand during continuous casting could intensify the problem. The described mechanisms that combines segregation (enhanced by the high content of S and P) and deformation explains the presence of the cracks identified in the slab structure in MZ zone. Cracks can be initiated in the brittle temperature range, when the accumulated strain exceeds the critical strain and/or the applied tensile stress exceeds the critical fracture stress during solidification [10].

C. *Microhardness and hardness tests*

Microhardness tests were carried out on the samples: SZ, MZ and CZ, applying a load of 25g. *Fig. 6*

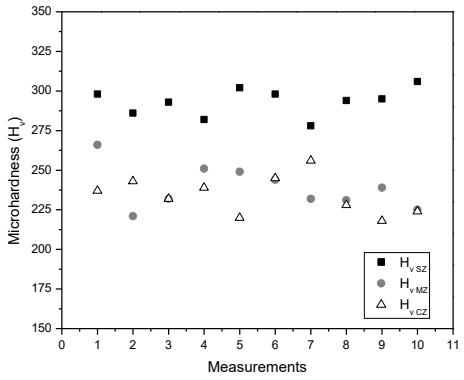

Fig. 6. *Resuls of microhardness measurements of SZ, MZ and CZ zones of the slab.*

The average microhardness value obtained in the shell zone of the slab is H_{vSZ} = 293, which is (≈ 18 %) higher than average values determined in the medium (MZ) and centre (CZ) zones, H_{vMZ} = 239 and H_{vCZ} = 234 respectively. This information shows the microhardness profile evolution from the surface to the centre of the slab. In the interdendritic zone a considerable increase of microhardness was obtained (H_v = 350), as result of segregation phenomena. Microhardness differences between dendritic grains and interdendritic zones indicates heterogeneity on mechanical behaviour in the slab, consistent with the presence of cracks in (MZ zone) between dendrites. Rockwell B hardness tests were performed and the average value obtained is H_{RB} = 64.5. On the base of hardness value, it was possible to estimate the equivalent value of tensile strength 370 N/mm2, consistent with the steel grade.

D. *Thermodynamic simulation*

The thermodynamic simulation of the AHSS steel was carried out applying Fact Sage 7.2, considering a temperature range of 1550ºC to 400ºC. Results make it possible to predict the phases evolution and precipitation phenomena at cooling conditions of the continuous casting process. At 1550ºC the steel system is completely liquid, contains B dissolved (B_L= $4.19.10^{-03}$ %wt) and low contents of FeS and MnS. At casting temperature (1530ºC) the steel is still liquid. At liquidus temperature T_L=1502ºC, estimated by (1), traces of the first solid phase (Fe_{BCC}, δ ferrite) is predicted. From T=1450ºC, the system is mainly constituted by solid phase (Fe_{FCC}, γ austenite) and low content of liquid phase. B and N (the last element in less amount), are dissolved as solutes in austenite. Also, TiN, TiC BN and BC start to precipitate in the solid phase. However, a considerable proportion of B remains dissolved in the liquid phase. The predicted chemical composition of the liquid phase is assumed as interdendritic liquid present in the system, see Table III. This result is consistent with the intergranular crack mechanisms mentioned for MZ zone which explain the crack propagation between dendrites because of the solute concentration increment in the interdendritic liquid. This is consistent with the high microhardness of the structure in the interdendritic zone. The presence of FeS also contributes to ductility loss promoting cracking problem during the solidification of the slab. When the temperature reaches ≈1400ºC, the steel becomes fully solid and the precipitation of CS_2Ti starts between austenite grain boundaries. Besides, TiN, TiC, BN and BC precipitation process in austenite grains continues.

TABLE III. INTERDENDRITIC LIQUID CHEMICAL COMPOSITION AT 1450ºC.

%Fe	%B	%C	%Mn	%N	%P	%Si
96.5	0.06	0.84	2.01	0.003	0.074	0.22
%Ti	%FeS	%MnS				
0.13	0.16	0.019				

Fig. 7 shows the evolution of the phases in the steel system during cooling in the continuous casting process.

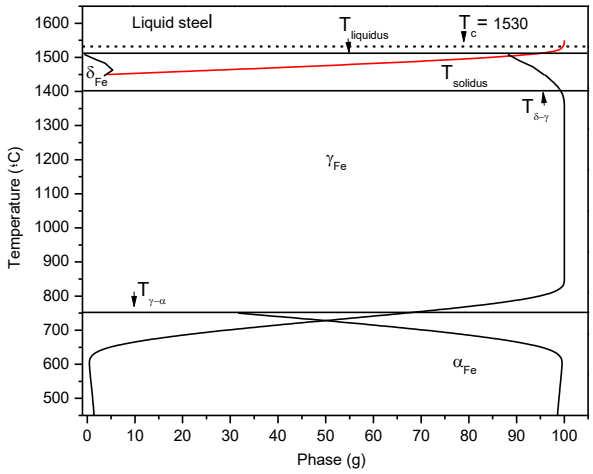

Fig. 7. *Resuls of phases transformation of the AHSS steel predicted by FactSage 7.2 simulation.*

Phases transformation temperatures constitute an important contribution for the continuous casting operation of this AHSS steel, in order to avoid defects and improve casting parameters during slab solidification. The predictions of temperature associated with phases transformations are: a) $T_{Liquidus \rightarrow \delta Fe}$= 1502ºC, b) $T_{\delta Fe \rightarrow \gamma Fe}$= 1450ºC and $T_{\gamma Fe \rightarrow \alpha Fe}$ = 750ºC. The casting temperature T_c= 1530ºC and the difference between the liquidus temperature and the casting temperature is ΔT= 28ºC.

It is known that boron is a strong nitride former [11]. Both things, B segregation and B nitrides or carbides precipitation in austenite grains retards γ→α transformation which improves final hardenability of AHSS steel through the adequate volume fraction of

martesite and bainite [1]. The solubility product for BN at 1050 to 1150 ºC is given by (2).

$$\log[\%B] = -2.45 \log[\%N] - 6.81 \quad (2)$$

In order to obtain a multiphase steel, with stable martesite and bainite phases it is necessary to maintain a high proportion of B free, as Fe_{FCC} (γ) solute, during the solidification [11]. Simulations results indicates that BC, BN precipitates compete with B and N dissolution in austenite grains from 1450ºC. When the system reaches T=1000ºC, Fe_2B (tetragonal) and BN precipitates also start to be formed between grain boundaries, and B dissolution (in austenite) is considerably decreased. The N solute in austenite decreases slowly during cooling.

The austenite grain boundary precipitation (BN, TiS2C and Fe2B) predicted during cooling in the steel by thermodynamic simulation occurs at temperatures $T \leq T_{solidus}$ and in austenite phase. The precipitation process between austenite grains continues at lower temperatures than T=750ºC, at which Fe_{BCC} (α) starts to nucleates in combination with carbon segregation, see *Fig. 7*

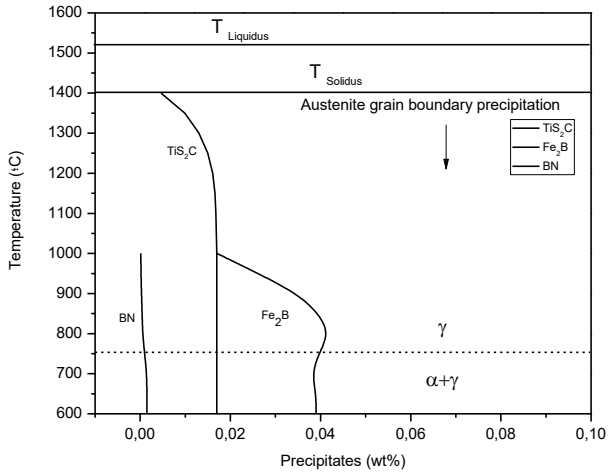

Fig. 8. *Prediction of austenite grain boundary precipitation during cooling.*

During the solidification, the boron element migrated to the grain boundary by means of the vacancy motion[12]. The migration velocity is very high, and the solubility of the boron in the grain boundary is low; therefore, the boride phases are easily precipitated.

The Fe_2B (tetragonal) promotes hardenability and it is formed in grain boundaries. The nucleation time (t_{inc}) was obtained by a linear regression (3) based on experimental data taken from Campos-Silva [13, 14]:

$$T_{inc}\ (s) = 2666.57 - 1.88xT \quad (3)$$

Applying (3) considering a temperature range of 1000ºC to 400ºC it is possible to predict that the precipitation of Fe_2B in the slab could be considered low and only at high temperatures, with a casting speed c_s=1 m/min.

It is relevant to take into account that at T= 1000ºC, the nucleation of Fe_2B starts and requires 270 (s) or 4.5 min of temperature maintenaince. During cooling the incubation time increase and at 400ºC the nucleation time is t_{inc}=1400 (s) or (23 min), see *Fig 9.*

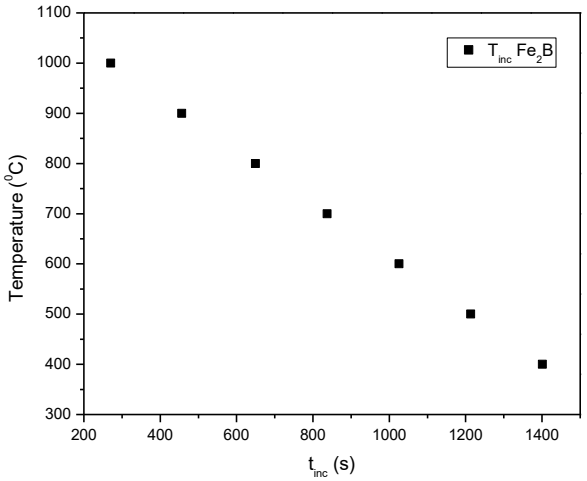

Fig. 9. *Fe_2B incubation time (T_{inc})at different temperatures conditions.*

By Fact Sage simulations, it was also possible to determine the different nature forms of boron in the system, at different cooling conditions: a) dissolved in the liquid steel, b) as solute in austenite and c) constituting different types of precipitates within grains or in the grain boundaries. According to Murari's study [1], in all the cases boron controls austenite transformation in relation with temperature during cooling. At fully austenized condition, B segregation and fine boron precipitation at austenite grain boundaries retards $\gamma \rightarrow \alpha$ transformation.

It is important to highlight that B atomic radius is 0.087 nm and for Fe is 0.126 nm. The ratio r_B / r_{Fe} is 0.69 which is between the required (acá falta un sustantivo: value?) for interstitial solid solution and substitutional solid solution. Taking into account/considering this ratio value, it is complex to stablish the B dissolution mechanism in austenite. Li in [15], estimated that the formation energy is lower when boron atoms occupy the octahedral sites and higher when boron atoms occupy the tetrahedron sites. For this reason, it is possible to deduce that boron diffuses to octahedral austenite sites. The alloy elements also affect B atoms diffusion in austenite.

In multiphase AHSS steel production, the amount of final martensite and bainite in the structure is controlled through boron content. According to [1], contents of B $\leq$ 0.0030 % increase the martesite volume fraction in relation witn bainite in the structure. On the contrary, B $\geq$ 0.0030 % results in structure with more bainite than martensite. On this base, the steel studied contains 0.0042 % B and could promote more bainite formation than martensite in the structure of the final product.

IV. CONCLUSIONS

The characterization study of the AHSS slab sample including non destructive tests (ultrasonic and penetrant liquid tests) combined with the structural study carried out by optical microscopy, scanning electron microscopy, hardness and microhardness tests allows to identify surface cracks in the shell (SZ zone), internal cracks in the dendritic zone (MZ) and segregation associated with porosity in the central zone (CZ) of the slab. The experimental results obtained through different techniques (destructine DT and non destructive NDT) are consistent and useful to improve the quality of the semifinished steel product. However, it is relevant to consider that ultrasonic signals are practical, economical and useful to examine bulk defects in slabs, avoiding interruptions or changes in the industrial production line.

The defects present in the slab sample are caused by multiple origins. Surface cracks (in SZ zone) are caused during the straightening operation that produces tension in the top surface of the strand at temperatures T≤ 1100ºC. The combination of tensile strain and low ductility may cause these surface cracks. In intermediate zone (MZ zone), cracks propagation is aligned with dendrites growth direction and is promoted by the increment of solute concentration in the interdendritic liquid. This is coincident with the high microhardness value obtained. Deformations owing to thermal gradients, ferrostatic pressure or rolls misalignment could intensify this type of cracks because of weakness of grain boundaries. Segregation and central porosity were also determined (in CZ zone) as a result of casting parameters alterations such as refrigeration problems or pressure changes in the extraction rolls during solidification.

The structural study determines the presence of MnS inclusions type I (globular), type II (dendritic) and type III (poligonal), due to a reaction in the interdendritic liquid. MnS type III affects the ductility behaviour. Also different precipitates are present in different zones of the slab sample: CNTi, TiC and TiS_2C. TiC are associated with complex silicates inclusions (size≈ 5µm). Microhardness measurements corroborate a considerable difference between the values of the grains in MZ and CZ zones (H_{vMZ} = 239 and H_{vCZ} = 234) and the interdendritic zone (H_v = 350) as a result of segregation phenomena consistent with interdendritic liquid chemical composition (predicted by Fact Sage simulation) and the cracks observed along grain boundaries.

Through thermodynamic simulation it was possible to determine the boron nature as austenite solute (in octahedrical sites) or constituting precipitates into grain austenite grains (BN, BC) or localized in grain boundaries (BN, Fe2B). It was possible to estimate that at casting conditions Fe2B precipitates in the slab structure are in low volume fraction. It was also corroborate the precipitation of TiS2C, TiC and BN in grain boundaries during cooling. Boron and precipitates help to control the ferrite nucleation in order to obtain the adequate volume fraction of bainite in the multiphase structure in this steel with 0.0042 ppm of B content. The simulation also brings phases transformation temperatures that constitute an important contribution for the continuous casting operation of this AHSS steel, in order to avoid defects and improve casting parameters during slab solidification.

ACKNOWLEDGMENT

The authors gratefully acknowledge the financial assistance of Universidad Tecnológica Nacional (UTN) under Project IPUTNSN0004951, from Argentina.

REFERENCES

[1] F.D. Murari, A.L. Vasconcellos da Costa e Silva and R. Ribeiro de Avillez, ″Cold rolled multiphase boron steels: microstructure and mechanical properties″, J. Mater. Res. Technol., vol. 4, 2, pp. 191-196, 2015.

[2] M. Tkadleckova, K. Michalek, K. Gryc, L. Socha, P Jonsta, M. Saternus, J. Pieprzyca and T. Merder, “Research and development of solidification of slab ingots frm special tool steels,” Arch. Metall. Mater., vol. 62, 3, pp. 1453-1458, 2017.

[3] W.R. Irving, ″Continuous casting of steel″. The Institute of Materials. London, 1983.

[4] C.W. Bale, P. Chartrand, S.A. Degterov, G. Eriksson and K.Hack, ″Fact Sage Thermomechanical Software and Databases″, CALPHAD, vol. 26, pp. 189-226, 2002.

[5] E. Brandaleze, M. Ramírez, M. Avalos, ″Microstructure Evolution at Different Cooling Rates of Low Carbon Microalloyed Steels″, Journal of Chemistry and Chemical Engineering, vol. 11, pp. 22-29, 2017.

[6] A.M. El-Wazri, F. Hassani, S. Yue, E. Es-Sadoi, L.E. Collins and K. Iibal, “The Effect of Thermal History on the Hot Ductility of Microalloyed Steels”, ISIJ International, vol. 39, 3, pp. 253-262, 1999.

[7] M.R. Allazadeh, C.I. Garcia, K.J. Alderson, and A.J. DeArdo, ″Using NDT Image Processing Analysis to Study the Soundness and Cleanliness of Accelerated Cooled Continuously Cast Steel Slabs″, Advanced Materials and Processes, vol. 166, 12, pp. 26-27, 2008.

[8] F. Zarandi and S. Yue, ″Mechanism for Loss of Hot Ductility Due to Deformation during Solidification in Continuous Casting of Steel″, ISIJ International, vol. 44, 10, pp. 1705-1713, 2004.

[9] N. Anmark, A. Karasev and P.G. Jönsson, ″The Effect of Differrent Non-metallic Inclusions on the Machinability of Steels″, Materials, vol. 8, pp. 751-783, 2015.

[10] Y.M. Won, H.N. Han, T. Yeo and K. H.OH, ″Analysis of Solidification Cracking Using the Specific

Crack Susceptibility″, ISIJ International, vol. 40, 2, pp. 271-350, 2000.

[11] F. Abe, ″Effect of Boron on Microstructure and Creep Strength of Advanced Ferritic Power Plant Steels″, Procedia Engineering, vol. 10, pp. 94-99, 2011.

[12] J.W. Li, G. Zhang, S. Wei and Q. Shao, “Preparation Technology of the Low Carbon High Boron Fe-C-B Wear Resistence Steel”, Applied Mechanics and Materials, vol. 52-54, pp. 1718-1722, 2011.

[13] M. Keddam, “An Approach for Analyzing the Growth Kinetics of Fe2B Phase on AISI 1018 Steel”, Defect and Diffusion Forum, vol. 297-301, pp. 269-274, 2010.

[14] J. Zuno-Silva, M. Ortiz-Domínguez, M. Keddam, M. E. Espinosa, O. D.Mejía, E. Cardoso-Legorreta, M. Abreu-Quijano, “Boriding Kinetics of Fe2B Layers Formed on AISI 1045 Steel”, J. Min. Metall. Sect. B-Metall, vol. 50-2B, pp. 101 – 107, 2014.

[15] X. Li, P. Wu, S. Zhao, C. Chen, R.Yin and N. Chen,″First – principle Study of the Solution Type of Borom in γ– iron″, Energy Procedia, vol. 16, pp. 661-666, 2012.